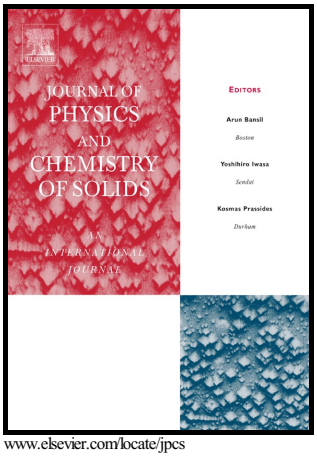

www.elsevier.com/locate/jpcs

$SbCl_3$ as effective catalyst for the preparation of 2,3-Dihydroquinazolin-4(1H)-ones, spectroscopic investigation and DFT study

Seied Ali Pourmousavi, Ayoob Kanaani, Hamid Reza Fatahi, Fatemeh Ghorbani, Davood Ajloo

PII: S0022-3697(16)30855-1
DOI: http://dx.doi.org/10.1016/j.jpcs.2017.03.008
Reference: PCS8006

To appear in: *Journal of Physical and Chemistry of Solids*

Received date: 9 October 2016
Revised date: 22 January 2017
Accepted date: 9 March 2017

Cite this article as: Seied Ali Pourmousavi, Ayoob Kanaani, Hamid Reza Fatahi Fatemeh Ghorbani and Davood Ajloo, $SbCl_3$ as effective catalyst for th preparation of 2,3-Dihydroquinazolin-4(1H)-ones, spectroscopic investigatio and DFT study, *Journal of Physical and Chemistry of Solids* http://dx.doi.org/10.1016/j.jpcs.2017.03.008

$SbCl_3$ as effective catalyst for the preparation of 2,3-Dihydroquinazolin-4(1*H*)-ones, spectroscopic investigation and DFT study

Seied Ali Pourmousavi[a,b*], Ayoob Kanaani[a], Hamid Reza Fatahi[a], Fatemeh Ghorbani[a], Davood Ajloo[a,b]

[a]*School of Chemistry, Damghan University, Damghan, 36715-364, Iran*

[b]*Institute of Biological Science, Damghan University, Damghan, 36716-41167, Iran*

[*]*Corresponding author. Tel.: +98-233-522-0097; fax: +98-233-522-0095; e-mail: pourmousavi@du.ac.ir.*

Abstract

A simple and efficient method has been developed for the synthesis of Quinazolines using $SbCl_3$ as a heterogeneous catalysis at room temperature. This method provides a good pathway for the synthesis of 2,3-Dihydroquinazolin-4(1*H*)-ones derivatives in the terms of excellent yields and short reaction times. Also we studied theoretically and experimentally on 2-phenyl-2,3-dihydroquinazolin-4(1H)-one (PDQ). Using density functional theory (DFT), the tautomerism of PDQ was also studied. Thermal stability of PDQ was studied by thermo gravimetric analysis (TGA). The spectroscopic results and theoretical calculations indicate that the strength of intramolecular hydrogen bonding (IHB) of PDQ is stronger than that in 2-methyl-4-quinolinol (2MQ). The absorption spectra of the PDQ in solvents with different polarity were obtained and the results show that PDQ exists in both keto-amine and enol-imine forms in THF, while it has keto-amine form in other solvents. Theoretical results show that the conductance of the two tautomers (keto-amine and enol-imine) varies greatly, which offers that the potential usage of this molecule is as a molecular device.

Keywords: 2-Aminobenzamide; 2,3-Dihydroquinazolin-4(1*H*)-ones; Catalyst; DFT

1.Introduction

The heterocyclic fused rings quinazolines have attracted a huge consideration because of their expanded applications in the field of pharmaceutical chemistry.[1-4] Many substituted quinazoline derivatives possess a wide range of bioactivities such as antimalarial,[5] anticancer,[6] antimicrobial,[7] antifungal,[8] antiviral,[9] antihypertensive,[10] anti-inflammatory,[11] anti-diabetes,[12] muscle relaxant,[13] antitubercular,[14] anti-

obesity,[15] anticonvulsant,[16] antiproliferative,[17] anti-oxidant,[18] and many other ones. Quinazolines compounds are used in preparation of various functional materials for the synthetic chemistry and also present in molecules of various drugs (Fig. S1).

Several synthetic routes have been widely used for the preparation of quinazoline derivatives. These compounds have been synthesized in the presence of a variety of homogeneous or heterogeneous catalysts such as molecular iodine (I_2),[19] cyanuric chloride,[20] morpholinoethanesulfonic acid,[21] silica supported polyphosphoric acid (SiO_2-PPA),[22] NH_4Cl,[23] tetrabutylammonium bromide (TBAB),[24] p-sulfonic acid calix[4]arene,[25] $[Al(H_2PO_4)_3]$,[26] β-cyclodextrin-SO_3H,[27] $[PYC_4SO_3H][HSO_4]$/A300SiO_2,[28] Fe_3O_4 nanoparticles,[29] [bmim]HSO_4,[30] $Sc(OTf)_3$,[31] cellulose-SO_3H,[32] β-cyclodextrin,[33] $ZrCl_4$,[34] Amberlyst-15,[35] $H_3PW_{12}O_{40}$,[36] Heteropoly Acids [37] or by electrochemical reactions.

These reported methods produce good results in many instances. However, some of them suffer from one or more drawbacks, including complex steps, prolonged reaction times, low yields and tedious work-up procedure and using expensive catalysts. Therefore, these compounds develop more efficient, rapid and simple procedures to prepare the similar skeleton compounds.

The use of antimony trichloride ($SbCl_3$) as catalyst has received considerable attention in organic synthesis, because it is cheap and easy to handle. $SbCl_3$ has shown a profound catalytic activity. As a Lewis acid, it has been used in organic synthesis such as Friedel-Crafts acylations,[38] reductions with $NaBH_4$ [39] and in the synthesis of some heterocycles.[40] To the best of our knowledge, there has been no such a report in the literature for the synthesis of quinazoline derivatives with $SbCl_3$ as a catalyst.

In continuation of our ongoing program to develop the new methodologies in organic synthesis, here we wish to report the extremely convenient and practical synthesis of 2,3-dihydroquinazolin-4(1*H*)-on derivatives *via* the simple and efficient condensation reaction of 2-aminobenzamide and aldehydes in the presence of a catalytic amount of $SbCl_3$ in MeOH.

Also, the tautomeric stability, optimized geometry, vibrational spectra, electronic absorption spectra, statistical thermodynamic parameters, molecular electrostatic potential, frontier molecular orbitals (FMOs), nonlinear optical properties, thermal stability and the electron transport properties based on the molecular switch of the 2-phenyl-2,3-dihydroquinazolin-4(1H)-one (PDQ), have been studied.

2.Experimental section:

2.1.General

The mid-IR spectrum was obtained using KBr pellets on a Perkin-Elmer RXI Fourier Transform spectrophotometer. The ultraviolet absorption spectra were examined in the range of 200–500 nm using Perkin-Elmer lambda 25 recording spectrophotometer equipped with a 10 mm quartz cell. The NMR Spectra were prepared at the ambient temperatures on Brucker AVANCE DRX-400 MHz spectrometer. Thermal analysis of TGA and DTG were performed on a Perkin–Elmer model under nitrogen at a heating rate of 10 °C/min for the temperature range of 100-800°C.

2.2.General procedure for the synthesis of quinazoline derivatives (1-16)

To a solution of 2-aminobezamide (1 mmol) and aldehyde or ketone (1 mmol) in MeOH (3 mL), $SbCl_3$ (0.03 gr) was added. The mixture was stirred at room temperature. After completion of the reaction, as indicated by TLC (ethyl acetate: n-hexane 1:1), the product was precipitated by addition of 9 mL of water. Then the precipitate was filtered off and washed with extra water. Finally the crude product was purified by recrystallization from EtOH and water to afford the corresponding 2,3-dihydroquinazolin-4-(1H)-ones.

2.3.Spectral data

2,3-dihydro-2- phenyl quinazolin-4(1*H*)-one (3a): ^{1}H NMR (400 MHz, DMSO): δ 5.75 (s, 1H), 6.67 (t, 1H), 6.76 (d, *J*= 8 Hz, 1H), 7.11 (s, 1H), 7.24 (t, 1H), 7.34-7.39 (m, 3H), 7.49 (d, *J*= 8 Hz , 2H), 7.61 (d, *J*= 6.4 Hz), 8.29 (s, 1H, br).

2,3-dihydro-2-(4-methoxy phenyl) quinazolin-4(1*H*)-one (3f): ^{1}H NMR (400 MHz, $CDC1_3$): δ 3.84 (s, 3H), 4.39 (s, 1H, br), 5.70 (s, 1H), 5.86-7.54 (m, 8H), 7.95 (s, 1H, br).

2,3-dihydro-2-(3,4- dimethoxy phenyl) quinazolin-4(1*H*)-one (3h): ^{1}H NMR (400 MHz, DMSO): δ 3.74 (s, 3H), 3.75 (s, 3H), 5.69 (s, 1H), 6.67 (t, 1H), 6.75 (dd, *J*= 8 Hz, 1H), 6.93-6.98 (m, 2H), 7.01 (s, 1H, br), 7.24 (m, 1H), 7.60 (dd, *J*= 8 Hz), 8.16 (s, 1H).

2,3-dihydro-2-(3,4,5-trimethoxy phenyl) quinazolin-4(1*H*)-one (3i): ^{1}H NMR (400 MHz, DMSO): δ 3.64 (s, 3H), 6.67-6.71 (m, *J*= 8 Hz, 1H), 6.76 (dd, *J*= 8 Hz, 1H), 6.84 (s, 2H), 7.04 (s, 1H, br), 7.26 (m, *J*= 8 Hz , 1H), 7.62 (s, *J*= 7.8 Hz ,1H), 8.21 (s, 1H). ^{13}C NMR (400 MHz, DMSO):

56.34, 60.34, 67.34, 104.86, 104.86, 114.89, 115.48, 117, 127.82, 133.75, 137.03, 137.03, 137.03, 137.97, 148.50, 153.18, 164.16.

3.Computational details

Quantum calculation chemistry has been quite successful in providing theoretical background of popular qualitative chemical concepts [41]. Quantum chemical calculations help chemist to calculate the structural and physicochemical properties of the molecule. With the encouraging experimental data of 2,3-dihydro-2-arylquinazolin-4(1H)-ones 3, our attention was focused on calculations for investigation of the physicochemical properties of 3a such as conformational studies, optimized geometry, vibrational analysis, intermolecular hydrogen bonding, molecular electrostatic potential (MEP) surface, UV–Vis spectra, electronic properties, Thermal analysis, transition state, current−voltage characteristics of linear switch.

The entire calculations for the PDQ have been done with a hybrid functional B3LYP at 6-311++G(d,p) basis set. We used, a higher computation level, such as B3LYP/6-311++G(2d,p), which allow a rationalization of these observations. All calculations were performed using Gaussian 03W program package [42] with the default convergence criteria without any constraint on the geometry.[43] The molecular structure of PDQ in the ground state was optimized. For all calculations in this study, optimized structural parameters were used. The vibrational frequencies were calculated and scaled down by the suitable scaling factor.[43] The vibrational wavenumber assignments were carried out by combining the results from the GaussView [44] and VEDA4 programs.[45] The Lorentzian function has been utilized for deconvolution of IR spectrum. Electronic excitations of PDQ were calculated using TD-DFT.[46] The polarizable continuum model (PCM) was used for solution phase calculations.[47] AIM 2000 software was applied to obtain the AIM computations.[48] The transition state (TS) structure of tautomeric reaction was obtained using the QST3 method.

The transport properties of the molecular junction were calculated using the TranSIESTA package [49] which is based on the combination of DFT with the nonequilibrium Green's function (NEGF) technique. In the lateral dimension, a 6×6 supercell was used, large enough to remove interactions between periodic images. Based on the experimental results, it is accepted that hydrogen atoms are not attached to metal surfaces.[50] According to this, the two hydrogen atoms which are to be connected to the metal surface were replaced with sulfur atoms, and the remaining portion was placed between two parallel Au(111) planes, which have a face-cantered cubic (FCC).

4. Results and Discussion

4.1. Synthesis of 2,3-dihydro-2-arylquinazolin-4(1H)-ones

A preliminary experiment was performed to determine the suitable reaction conditions. The reaction of 2-aminobezamide and 4-Methyl benzaldehyde in the presence of $SbCl_3$ was investigated. The best result was obtained in the presence of 0.03 gr $SbCl_3$ at room temperature in MeOH (Table 1).

The yield of **3b** was low at r.t. in the absence of $SbCl_3$ (10%, Table 1, entry 6), and was much greater in the presence of various quantities of the catalyst, reaching to a maximum of 100% yield with 0.03 gr $SbCl_3$ (Table 1, entries 3). Different solvents were also tested (Table 1, entries 7-14), and MeOH appeared to be the best medium for this transformation (Scheme).

These optimized conditions were applied to the conversion of various kinds of aryl aldehydes or ketones into the 2,3-dihydro-2-arylquinazolin-4(1H)-ones. All of reactions that are done using aldehydes containing electron-withdrawing or electron-donating groups, proceeded smoothly within a few mins, giving **3a**-**p** (Table 2). The products were synthesized in good to excellent yields and characterized by ^{1}H-NMR, ^{13}C-NMR, as well as by their physical constants. To further evaluate the overall utility of the current methodology, we compared our results with those obtained using other techniques previously reported for the synthesis of 2,3-dihydro-2-arylquinazolin-4(1*H*)-ones. As shown in Table 3, our both methods clearly reduce the required reaction time and generate higher yields of the products.

4.2.Conformational studies and optimized geometry

All optimization calculations for PDQ were performed by aid of OPT=Very Tight and INT=Ultrafine options. DFT calculations were performed for three tautomers of PDQ (Fig. 1). The calculated relative energies in gas and solution phases are presented in Table S1. The keto-amine (I) tautomer form is more stable than the enol-imine (II) and Enol-amine (III) tautomers by 11.30 and 34.38 kcal/mol in gas phase, which these amounts increase with increasing the polarity of solvent. According to Table S1, the keto-amine and the enol-imine forms have the highest and lowest dipole moment amounts, respectively.

The calculated IR spectra for different I-III configurations of PDQ at B3LYP-/6-311++G(2d,p) level of theory are shown in Figs. S2, S3. The stretching and bending modes of C=O, which were observed experimentally, do not detected in calculated IR spectra at configurations II and III. Also, there is a peak in the high-frequency region, which is not seen

in the experimental results. This peak is assigned to the stretching vibration of OH. In these configurations (II, III), the observed bands corresponding to δO-H, υC=N and υC–O vibrations, have not seen in the experimental spectrum. These results confirmed that our PDQ is stable at the keto-amine form.

Geometric optimization of PDQ was performed using DFT/B3LYP method with 6-311++G(2d,p) basis set (Fig. 2). The selected torsion angles, bond angles and bond lengths are listed in Table 4. The results are compared with another similar system in which the crystal structure was solved.[51]

Because of the hydrogen bonding formation, dimerization of PDQ considerably reduces the energy about -50.26 kJ/mol (at the B3LYP/6-311++G(d,p). The energy difference between dimer and keto forms suggests that there is a hydrogen bond in the dimeric form (Fig. S4). The O...H distance in hydrogen bonded dimer is found to be 1.770 Å. The N–H and C=O distances involved in hydrogen bonds are lengthened by 0.025 and 0.022 Å respectively upon dimerization.

The bond lengths of C_3–N_{15}=1.389 Å, C_{10}–N_{16}=1.361 Å, C_{13}–N_{16}=1.461 Å and C_{13}–N_{15}=1.463 Å are shorter than the normal C–N single bond length of about 1.48 Å, which this shortening indicates a resonance in this part of the molecule.[52] For PDQ, it is found that the carbon-carbon bond lengths in the benzene ring are between generic C=C double (1.34 Å) and C–C single (1.54 Å) bonds lengths. The greater bond length of C_3–C_4 (1.409Å) is a result of delocalization of electron density with adjacent quinazoline ring. The calculated value of C=O bond length (1.243 Å) in PDQ dimer reported in Table 4 is in good agreement with experimental data.

The ortho and mono substituted phenyl rings are designated as rings I and II, respectively. For PDQ, the dihedral angles are C_5–C_4–C_{10}–N_{16}= -175.5º and C_{10}–N_{16}–C_{13}–C_{18}= -166.1º. This shows that the phenyl ring I and the quinazoline moiety of PDQ are in tilted situation. Also, the dihedral angles C_{13}–C_{18}–C_{20}–C_{23}, C_{18}–C_{13}–N_{15}–C_3, and C_{18}–C_{13}–N_{16}–C_{10} are -179.5º, 172.2º and -176.1º, respectively, which indicate the phenyl ring II and the quinazoline moiety are not in the same plane.

None of three bond angles around C_{10} atom are equal to 120º. It is seen that the angle C_4–C_{10}–O_{17} (122.1º) is considerably greater than the angle N_{16}–C_{10}–C_4 (115.6º), which can be explained because of a decline in the repulsion among the lone pairs existing in N_{16} and O_{17} atoms.

4.3.Vibrational analysis

The PDQ molecule contains 29 atoms, which has 81 normal modes of fundamental vibrations. The experimental and calculated FT-IR spectra of PDQ in the region of 4000–400 cm^{-1} are shown in Fig. 3 (a) and (b), respectively. In order to clarify the observation of these bands, the band deconvolution technique is used in the IR spectrum. The deconvoluted IR spectrum of PDQ is demonstrated in Fig. S5. The value of the correlation coefficient provides good linearity between the calculated and experimental wavenumbers (R^2=0.9973) and is shown in Fig. S6 in Supplementary.

In PDQ, the calculated C=O stretching vibration is at 1726 cm^{-1} and a strong band is observed in IR spectrum at 1671 cm^{-1} (Table 5). The dominant in-plane C=O bending vibration in the case of PDQ is calculated at 599 cm^{-1} in complete consistency with Rastogi et al.[53]

In this study, the theoretical calculation presents that the values of the scaled frequencies at 3438 and 3423 cm^{-1} are assigned to N–H stretching vibrations. The PED corresponding to these vibrations are pure modes with a contribution of 100 %. These bands are observed at 3301 and 3178 cm^{-1} in FT-IR spectrum as a medium band.

In the present study, the frequencies observed in the FT-IR spectrum at 1587, 1439, 1427, 1362 cm^{-1} are assigned to N–H in-plane bending vibrations. Considering the N–H out-of-plane bending vibrations, medium to week FT-IR bands are assigned at 641, 600 and 565 cm^{-1}. These assignments are in agreement with the literature.[54]

Tanak et al.[55] assigned C–N stretching absorption in the region of 1339–1151 cm^{-1} for aromatic amines. In the present work, the bands observed in the region of 1284–1134 cm^{-1} in FT-IR spectrum are assigned to C–N stretching vibrations. These modes are not pure but contain significant contributions from other modes.

For ortho substituted benzene, the υPh modes are expected to be in the range of 1620–1260 cm^{-1} and for mono substituted benzene these modes are seen in the region of 1285–1610 cm^{-1}.[56] For ring Ph I, the υPh modes are observed at 1660, 1587, 1510, 1327 cm^{-1} experimentally and at 1642, 1612, 1520, 1342 cm^{-1} theoretically and for ring Ph II, are observed at 1649, 1613, 1301 cm^{-1} experimentally and at 1638, 1621, 1310 cm^{-1} theoretically. The ring breathing mode of PDQ is assigned at 1075 cm^{-1} for ring Ph I and at 1035 cm^{-1} for ring Ph II by PED calculations. The bands occurring at 922, 852, 727 and 664 cm^{-1} in infrared are assigned to CCC in-plane bending modes of PDQ. The bands are assigned to CCC out-of-plane bending vibrations are observed at 529, 508 and 490 cm^{-1} in PDQ.

The C–H stretching vibrations are calculated at 3056–3016 cm^{-1}. These vibrations are in good agreement with the experimental values. For example, the experimental value is appeared at 3035 cm^{-1} and the calculated one is obtained at 3045 cm^{-1}. As can be seen from the Potential Energy Distribution (PED) column shown in Table 5, these modes are pure. The in-plane and out of plane C–H bending vibrations emerge in the range 1000–1300 cm^{-1} and 750–1000 cm^{-1}, respectively. As an example, the emergence of C–H out of plane bending vibration (or wagging) modes started from 985 cm^{-1} and distributed up to 699 cm^{-1}, whereas these are predicted in the region of 987–712 cm^{-1}.

4.4.Intermolecular hydrogen bonding

Some optimized geometrical parameters, AIM results and the spectroscopic properties related to the hydrogen bond strength for PDQ and 2-methyl-4-quinolinol (2MQ) [57] are listed in Table 6. By comparing these properties, the following trend in hydrogen bond strength is concluded: PDQ > 2MQ

According to Table 6, the values of O…N and O…H distances decrease, while the NHO bond angle and N-H bond length in PDQ increase compared to 2MQ. This is in agreement with the AIM results (see Table 6). The electron density at bond critical point (ρ_{BCP}) in PDQ is greater than that of in 2MQ. Thus, it is evidence showing that IHB in PDQ is stronger than 2MQ. The values of the hydrogen bond energy (E_{HB}) for PDQ (13.54) and 2MQ (7.08), are calculated and reported in Table 6, which is in agreement with the above trend for IHB strength. This is confirmed by studying the IR frequencies of PDQ. PDQ, compared to 2MQ, has smaller N_{16}-H_{14} stretching frequency (3438 cm^{-1}) and bigger out-of-plane bending frequency (571 cm^{-1}).

4.5.Molecular electrostatic potential (MEP) surface

To predict reactive sites for electrophilic and nucleophilic attacks for PDQ, the MEP at B3LYP/6-311++G(2d,p) method is calculated. The red and yellow[1] (negative) and the blue (positive) areas of MEP are linked to electrophilic and nucleophilic reactivity. It can be concluded from Figure 4 that the negative territory of the compound is concentrated around the carbonyl O_{17} atom. The maximum value of negative electrostatic potential for this electrophilic site calculated at B3LYP/6-311++G(2d,p) is about -22.410 a.u with point charge

[1] For interpretation of colour in Fig. 4, the reader is referred to the web version of this article.

-0.618 e. For the feasible nucleopilic reaction, the maximum positive regions are located on hydrogen atoms bonded to N atoms. These sites give information about the regions in which the compound can have intermolecular interactions.

4.6.UV–Vis spectra and electronic properties

Gauss-Sum 2.2 program [58] is used to calculate group contributions to the molecular orbitals (HOMO and LUMO) and provide the density of the states (DOS), as shown in Fig. S7. DOS plot shows population analysis per orbital and indicates an easy outlook of the makeup of the molecular orbitals in a certain energy range. The energy gap between HOMO and LUMO characterizes the molecular chemical stability, softness, hardness and chemical reactivity of the molecule. [59] For PDQ, the energy difference between HOMO and LUMO is 4.6856 eV (see Fig. 5).

Experimental UV–vis spectra of PDQ in five organic solvents with different polarities (CH_2Cl_2, C_2H_5OH, THF, CH_3OH and CH_3CN) are shown in Fig. 6. The experimental spectrum shows three bands at 330, 261 and 219 nm (in CH_3CN).

The absorption spectra of this compound is characterized by intense absorption peaks near 200–250 nm and the less intense ones around 290–400 nm. The band in the region 290–400 nm is due to π–π* transition attributed to the conjugated quinoline ring of the molecule in analogy with the assignment for π-styrylquinolines [60], whereas the lowest energy band which is largely of charge transfer character is due to the aryl group. The band observed in 205 nm unacceptable, because it is less than UV cutoff for THF solvent.

However, a new absorption band at 368 nm is observed in the spectrum of PDQ in THF (Fig. 6), which is not present in the case of the other solvents. The enol-imine form becomes important in the solution and is stabilized by the less polar solvent. The electron donating phenyl group stabilizes zwitter ionic form and eases the formation of enol-imine form with resonance. In addition, the formation of enol-imine form can be related to the polarity of solvent. According to Table S1, the enol-imine form has the lowest dipole moment amount. Among the solvents used in this work, THF has the lowest polarity amount. This property causes both keto-amine and enol-imine forms to be stable in the solvent.

In addition, the first 10 spin-allowed singlet–singlet excitations for both keto-amine and enol-imine forms are calculated by TD-DFT approach. For both keto-amine and enol-imine forms of PDQ, wavelength (λ), oscillator strength (*f*) and major contributions of calculated transitions are given in Table 7. There is good agreement between theoretical and

experimental results. For keto form the charge transfer band at $\lambda_{cal.}$ 239 nm results mainly (46%) due to an electronic transition from HOMO to LUMO+4. smaller contributions (20%, 12%) to these states are attributed to electronic transition from HOMO-2 to LUMO and HOMO-1 to LUMO. The HOMO and LUMO are mainly localized on the 2,3-Dihydroquinazolin-4(1H)-one and the whole molecule, respectively (see Figure 5). The bands calculated at. 270 and 324 nm are due to one electronic transitions from HOMO to LUMO+1 (96%) and from HOMO to LUMO (97%), respectively. Also, the major contributions from enol form are listed in table 7.

4.7.Thermal analysis

Thermal analysis of PDQ is carried out using the Perkin–Elmer model and simultaneous thermo gravimetric/differential thermal (TG/DT) analyzer. The sample is scanned in the temperature range of 100–800 °C at a rate of 10 °C/min. The TG/DT curve is shown in Fig. 7. The major weight loss (80%) take occurs between 270 °C and 378 °C. In the differential thermal gravimetry (DTG) curve, one peak is identified at temperature of 324 °C, indicating that the weight loss caused by thermal decomposition occurs in one step, presumably due to the decomposition of functional groups and carbonization (Fig. 7). This TGA and DTG show that PDQ compound is chemically stable up to 324 °C.

4.8. Transition state and kinetic

The transition state (TS) structure of tautomer equilibrium (I↔II) gained to use QST3 method and optimized structure is shown in Fig. S8. The imaginary frequency that characterizes the TS is mainly associated with the hydrogen transfer from O_{17} to the N_{16}. Intrinsic reaction coordinate (IRC) calculations are accomplished to confirm that the transition state structures connect the reactant and product during the reaction (Fig. S9). Frequency calculations provide thermodynamic parameters to approximate activation parameters; the results are given in Table S2.

The first order rate constant *k*(T) is calculated using the transition state theory (TST).[61] In order to evaluate the effect of temperature on the reaction rate, reaction rate constants (k) are calculated in the temperature range of 250–450 K. The value of activation energy is obtained from the plot of calculated (–log*k*) vs. 1000/T. $\overline{E_a}$ is obtained from the slope of plot and the data are presented in Table S3. By increasing the temperature, the rate constant

increased too. When the temperature changed from 250 K to 450 K, *k* increased approximately 10^{15} times.

One way to obtain the most stable tautomer is to calculate the tautomeric equilibrium constant, K_{eq}, which is readily calculated from the Gibb's free energy via $K_{eq}=e^{-\Delta G/RT}$.[62] The ΔG value at the B3LYP/6-311++G(d,p) level is predicted to be 49.208 kJ/mol between keto-amine and enol-imine tautomers of PDQ. The computed K_{eq} is 2.703×10^{-9} at 298.15 K for keto-amine ↔ enol-imine tautomerization. This result demonstrates that the direction of equilibrium is in favor of the keto-amine tautomeric form.

4.9.Current−Voltage Characteristics of Linear Switches

The structural optimization is accomplished in the SIESTA package[49] with the maximum force of 0.02 eV/Å, and core electrons are modeled using Troullier-Martins[63] soft norm-conserving pseudo potentials. The Perdew–Burke–Ernzerhof (PBE) exchange–correlation functional is adopted for the generated gradient approximation (GGA).[64] The Au atoms are described as a single-ξ plus single polarization (SZP) basis set while for the other atoms a double-ξ plus single polarization (DZP) basis set is used. The current through the device is computed using the Landauer–Büttiker formula in the TranSIESTA package.[49]

As illustrated in Fig. S10, the whole device is divided into three regions, the right electrode, the central scattering region, and the left electrode. Fig. 8 shows the calculated I–V characteristics of the system with two forms (keto-amine, enol-imine) at a bias up to 2 V. The switching action can be obviously seen in Fig. 8; the current of keto-amine form is greater than that of enol-imine form at the same bias. It can be predicted that there is a switch from the *on* (low resistance) state to the *off* (high resistance) state when the keto-amine form is changed to the enol-imine form.

5. Conclusion

In summary, we have developed an efficient methodology for the synthesis of a variety of 2,3-dihydro-2-arylquinazolin-4(1H)-one derivatives in excellent yields. This approach is very simple from the experimental point of view and would permit easy access to large families of quinazolin-4(1H)-ones. Our work is clean, efficient and mild with short reaction times and easy purification. Minimized amount of waste for each organic transformation and economic availability of the catalyst are the other noticeable features of this method. Also, this paper

presents a combined experimental and theoretical study on 2-phenyl-2,3-dihydroquinazolin-4(1H)-one (PDQ). FT-IR spectra analysis showed that the vibrational frequencies are in nice agreement with the experimental values. PDQ compound is chemically stable up to 324 °C. The experimental (IR) and theoretical (AIM and geometrical parameters) results confirmed that the hydrogen bond in PDQ is stronger than that in 2MQ. UV-vis spectra of PDQ were recorded in different organic solvents in order to peruse the dependence of tautomerism on solvent types. The results showed that PDQ exists in both keto-amine and enol-imine forms in THF, while it has only keto-amine form in C_2H_5OH, CH_2Cl_2, CH_3OH and CH_3CN. The computed tautomeric equilibrium constant was 2.703×10^{-9} at 298.15 K for keto-amine ↔ enol-imine tautomerization. Our results showed that the conductance of two isomers varies greatly, which offers that the potential usage of this molecule is as a molecular switch.

Acknowledgments

Authors are grateful to the Damghan University for financial support.

References

[1] S.B. Mhaske, N.P. Argade, The chemistry of recently isolated naturally occurring quinazolinone alkaloids, Tetrahedron, 62 (2006) 9787-9826.

[2] J.-F. Liu, Rapid syntheses of biologically active quinazolinone natural products using microwave technology, Current Organic Synthesis, 4 (2007) 223-237.

[3] D.J. Connolly, D. Cusack, T.P. O'Sullivan, P.J. Guiry, Synthesis of quinazolinones and quinazolines, Tetrahedron, 61 (2005) 10153-10202.

[4] P. Griess, Ueber die Einwirkung von Cyan auf Amidobenzoësäure und Anthranilsäure in Wässeriger Lösung, Berichte der deutschen chemischen Gesellschaft, 11 (1878) 1985-1988.

[5] Y. Takaya, H. Tasaka, T. Chiba, K. Uwai, M.-a. Tanitsu, H.-S. Kim, Y. Wataya, M. Miura, M. Takeshita, Y. Oshima, New type of febrifugine analogues, bearing a quinolizidine moiety, show potent antimalarial activity against Plasmodium malaria parasite, Journal of medicinal chemistry, 42 (1999) 3163-3166.

[6] Y. Xia, Z.-Y. Yang, M.-J. Hour, S.-C. Kuo, P. Xia, K.F. Bastow, Y. Nakanishi, P. Nampoothiri, T. Hackl, E. Hamel, Antitumor agents. Part 204: synthesis and biological evaluation of substituted 2-aryl quinazolinones, Bioorganic & medicinal chemistry letters, 11 (2001) 1193-1196.

[7] R.J. Alaimo, H.E. Russell, Antibacterial 2, 3-dihydro-2-(5-nitro-2-thienyl) quinazolin-4-(1H)-ones, Journal of medicinal chemistry, 15 (1972) 335-336.

[8] M.-J. Hour, L.-J. Huang, S.-C. Kuo, Y. Xia, K. Bastow, Y. Nakanishi, E. Hamel, K.-H. Lee, 6-Alkylamino-and 2, 3-dihydro-3'-methoxy-2-phenyl-4-quinazolinones and related compounds: their synthesis, cytotoxicity, and inhibition of tubulin polymerization, Journal of medicinal chemistry, 43 (2000) 4479-4487.

[9] H. Li, R. Huang, D. Qiu, Z. Yang, X. Liu, J. Ma, Z. Ma, Synthesis and bioactivity of 4-quinazoline oxime ethers, Progress in Natural Science, 8 (1998) 359-365.

[10] E. Honkanen, A. Pippuri, P. Kairisalo, P. Nore, H. Karppanen, I. Paakkari, Synthesis and antihypertensive activity of some new quinazoline derivatives, Journal of medicinal chemistry, 26 (1983) 1433-1438.

[11] A. Baba, N. Kawamura, H. Makino, Y. Ohta, S. Taketomi, T. Sohda, Studies on Disease-Modifying Antirheumatic Drugs: Synthesis of Novel Quinoline and Quinazoline Derivatives and Their Anti-inflammatory Effect 1, Journal of medicinal chemistry, 39 (1996) 5176-5182.

[12] M.S. Malamas, J. Millen, Quinazolineacetic acids and related analogs as aldose reductase inhibitors, Journal of medicinal chemistry, 34 (1991) 1492-1503.

[13] N.P. Abida, M. Arpanarana, An updated review: newer quinazoline derivatives under clinical trial, International Journal of Pharmaceutical & Biological Archive, 2 (2011) 1651-1657.

[14] P. Nandy, M. Vishalakshi, A. Bhat, Synthesis and antitubercular activity of Mannich bases of 2-methyl-3H-quinazolin-4-ones, Indian Journal of heterocyclic chemistry, 15 (2006) 293-294.

[15] S. Sasmal, G. Balaji, H.R.K. Reddy, D. Balasubrahmanyam, G. Srinivas, S. Kyasa, P.K. Sasmal, I. Khanna, R. Talwar, J. Suresh, Design and optimization of quinazoline derivatives as melanin concentrating hormone receptor 1 (MCHR1) antagonists, Bioorganic & medicinal chemistry letters, 22 (2012) 3157-3162.

[16] Y. Kurogi, Y. Inoue, K. Tsutsumi, S. Nakamura, K. Nagao, H. Yoshitsugu, Y. Tsuda, Synthesis and hypolipidemic activities of novel 2-[4-[(diethoxyphosphoryl) methyl] phenyl] quinazolines and 4 (3 H)-quinazolinones, Journal of medicinal chemistry, 39 (1996) 1433-1437.

[17] M. Fares, W.M. Eldehna, S.M. Abou-Seri, H.A. Abdel-Aziz, M.H. Aly, M.F. Tolba, Design, Synthesis and In Vitro Antiproliferative Activity of Novel Isatin-Quinazoline Hybrids, Archiv der Pharmazie, 348 (2015) 144-154.

[18] G. Saravanan, V. Alagarsamy, C.R. Prakash, Synthesis and evaluation of antioxidant activities of novel quinazolinone derivatives, Int J Pharm Pharm Sci, 2 (2010) 83-86.

[19] X.-S. Wang, J. Sheng, L. Lu, K. Yang, Y.-L. Li, Combinatorial synthesis of 3-arylideneaminoquinazolin-4 (1 H)-one derivatives catalyzed by iodine in ionic liquids, ACS combinatorial science, 13 (2011) 196-199.

[20] M. Sharma, S. Pandey, K. Chauhan, D. Sharma, B. Kumar, P.M. Chauhan, Cyanuric chloride catalyzed mild protocol for synthesis of biologically active dihydro/spiro quinazolinones and quinazolinone-glycoconjugates, The Journal of organic chemistry, 77 (2012) 929-937.

[21] V.B. Labade, P.V. Shinde, M.S. Shingare, A facile and rapid access towards the synthesis of 2, 3-dihydroquinazolin-4 (1H)-ones, Tetrahedron Letters, 54 (2013) 5778-5780.

[22] M.R.M. Shafiee, One-pot preparation of N, N′-alkylidene bisamide derivatives catalyzed by silica supported polyphosphoric acid (SiO 2-PPA), Journal of Saudi Chemical Society, 18 (2014) 115-119.

[23] A. Shaabani, A. Maleki, H. Mofakham, Click Reaction: highly efficient synthesis of 2, 3-dihydroquinazolin-4 (1 H)-ones, Synthetic Communications®, 38 (2008) 3751-3759.

[24] M.A.B. Fard, A. Mobinikhaledi, M. Hamidinasab, An Efficient One-Pot Synthesis of 2, 3-dihydroquinazolin-4 (1H)-ones in Green Media, Synthesis and Reactivity in Inorganic, Metal-Organic, and Nano-Metal Chemistry, 44 (2014) 567-571.

[25] M. Rahman, I. Ling, N. Abdullah, R. Hashim, A. Hajra, Organocatalysis by p-sulfonic acid calix [4] arene: a convenient and efficient route to 2, 3-dihydroquinazolin-4 (1 H)-ones in water, RSC Advances, 5 (2015) 7755-7760.

[26] H.R. Shaterian, A.R. Oveisi, M. Honarmand, Synthesis of 2, 3-dihydroquinazoline-4 (1 H)-ones, Synthetic Communications®, 40 (2010) 1231-1242.

[27] J. Wu, X. Du, J. Ma, Y. Zhang, Q. Shi, L. Luo, B. Song, S. Yang, D. Hu, Preparation of 2, 3-dihydroquinazolin-4 (1 H)-one derivatives in aqueous media with β-cyclodextrin-SO 3 H as a recyclable catalyst, Green Chemistry, 16 (2014) 3210-3217.

[28] G. Yassaghi, A. Davoodnia, S. Allameh, A. Zare-Bidaki, N. Tavakoli-Hoseini, Preparation, characterization and first application of aerosil silica supported acidic ionic liquid as a reusable heterogeneous catalyst for the synthesis of 2, 3-dihydroquinazolin-4 (1H)-ones, Bulletin of the Korean Chemical Society, 33 (2012) 2724-2730.

[29] Z.-H. Zhang, H.-Y. Lü, S.-H. Yang, J.-W. Gao, Synthesis of 2, 3-dihydroquinazolin-4 (1 H)-ones by three-component coupling of isatoic anhydride, amines, and aldehydes

catalyzed by magnetic Fe3O4 nanoparticles in water, Journal of combinatorial chemistry, 12 (2010) 643-646.

[30] N.B. Darvatkar, S.V. Bhilare, A.R. Deorukhkar, D.G. Raut, M.M. Salunkhe, [bmim] HSO4: an efficient and reusable catalyst for one-pot three-component synthesis of 2, 3-dihydro-4 (1 H)-quinazolinones, Green Chemistry Letters and Reviews, 3 (2010) 301-306.

[31] J. Chen, W. Su, H. Wu, M. Liu, C. Jin, Eco-friendly synthesis of 2, 3-dihydroquinazolin-4 (1 H)-ones in ionic liquids or ionic liquid–water without additional catalyst, Green Chemistry, 9 (2007) 972-975.

[32] B.S. Reddy, A. Venkateswarlu, C. Madan, A. Vinu, Cellulose-SO 3 H: an efficient and biodegradable solid acid for the synthesis of quinazolin-4 (1H)-ones, Tetrahedron Letters, 52 (2011) 1891-1894.

[33] K. Ramesh, K. Karnakar, G. Satish, B.A. Kumar, Y. Nageswar, A concise aqueous phase supramolecular synthesis of 2-phenyl-2, 3-dihydroquinazolin-4 (1H)-one derivatives, Tetrahedron Letters, 53 (2012) 6936-6939.

[34] M. Abdollahi-Alibeik, E. Shabani, Synthesis of 2, 3-dihydroquinazolin-4 (1H)-ones catalyzed by zirconium (IV) chloride as a mild and efficient catalyst, Chinese Chemical Letters, 22 (2011) 1163-1166.

[35] S.B. Bharate, N. Mupparapu, S. Manda, J.B. Bharate, R. Mudududdla, R.R. Yadav, R.A. Vishwakarma, Efficient synthesis of 2, 3-dihydroquinazolin-4 (1H)-ones using heterogeneous solid acid catalysts: unexpected formation of, Arkivoc, 8 (2012) 308-318.

[36] Y. Zong, Y. Zhao, W. Luo, X.H. Yu, J.K. Wang, Y. Pan, Highly efficient synthesis of 2, 3-dihydroquinazolin-4 (1H)-ones catalyzed by heteropoly acids in water, Chinese Chemical Letters, 21 (2010) 778-781.

[37] N. Azizi, L. Torkiyan, M.R. Saidi, Highly efficient one-pot three-component Mannich reaction in water catalyzed by heteropoly acids, Organic letters, 8 (2006) 2079-2082.

[38] S. Mazières, C. Le Roux, M. Peyronneau, H. Gornitzka, N. Roques, Structural Characterization of Bismuth (III) and Antimony (III) Chlorotriflates: Key Intermediates in Catalytic Friedel− Crafts Transformations, European Journal of Inorganic Chemistry, 2004 (2004) 2823-2826.

[39] S. Sayama, Y. Inamura, Conjugate reduction of 2-butene-1, 4-diones with LiAlH4-SbCl3, Bulletin of the Chemical Society of Japan, 64 (1991) 306-308.

[40] Q. Wu, Y. Wang, W. Chen, H. Liu, Mild, efficient, and selective cleavage of trityl ethers with antimony trichloride, Synthetic communications, 36 (2006) 1361-1366.

[41] P. Geerlings, F. De Proft, W. Langenaeker, Conceptual density functional theory, Chemical reviews, 103 (2003) 1793-1874.

[42] M. Frisch, G. Trucks, H. Schlegel, G. Scuseria, M. Robb, J. Cheeseman, J. Montgomery Jr, T. Vreven, K. Kudin, J. Burant, Gaussian 03, revision B. 05; Gaussian, Inc., Pittsburgh, PA, (2003) 12478.

[43] M. Karabacak, M. Cinar, M. Kurt, Molecular structure and vibrational assignments of hippuric acid: A detailed density functional theoretical study, Spectrochimica Acta Part A: Molecular and Biomolecular Spectroscopy, 74 (2009) 1197-1203.

[44] A. Frisch, A. Nielsen, A. Holder, Gaussview users manual, Gaussian Inc., Pittsburgh, PA, (2000).

[45] M.H. Jamróz, Vibrational energy distribution analysis (VEDA): scopes and limitations, Spectrochimica Acta Part A: Molecular and Biomolecular Spectroscopy, 114 (2013) 220-230.

[46] M.E. Casida, K.C. Casida, D.R. Salahub, Excited-state potential energy curves from time-dependent density-functional theory: A cross section of formaldehyde's 1A1 manifold, International journal of quantum chemistry, 70 (1998) 933-941.

[47] J. Tomasi, M. Persico, Molecular interactions in solution: an overview of methods based on continuous distributions of the solvent, Chemical Reviews, 94 (1994) 2027-2094.

[48] R.F. Bader, Atoms in molecules, Wiley Online Library, 1990.

[49] M. Brandbyge, J.-L. Mozos, P. Ordejón, J. Taylor, K. Stokbro, Density-functional method for nonequilibrium electron transport, Physical Review B, 65 (2002) 165401.

[50] A.C. Van Duin, A. Strachan, S. Stewman, Q. Zhang, X. Xu, W.A. Goddard, ReaxFFSiO reactive force field for silicon and silicon oxide systems, The Journal of Physical Chemistry A, 107 (2003) 3803-3811.

[51] L. Zhang, J. Li, X. Yang, D. Shi, J. Chen, 2-Methyl-2-phenyl-1, 2-dihydroquinazolin-4 (3H)-one, Acta Crystallographica Section E: Structure Reports Online, 64 (2008) o450-o450.

[52] H. Arslan, U. Flörke, N. Külcü, G. Binzet, The molecular structure and vibrational spectra of 2-chloro-N-(diethylcarbamothioyl) benzamide by Hartree–Fock and density functional methods, Spectrochimica Acta Part A: Molecular and Biomolecular Spectroscopy, 68 (2007) 1347-1355.

[53] V. Rastogi, M. Palafox, K. Lang, S. Singhal, R. Soni, R. Sharma, Vibrational spectra and thermodynamics of biomolecule: 5-chlorocytosine, Indian Journal of Pure and Applied Physics, 44 (2006) 653.

[54] J. Evans, The vibrational assignments and configuration of aniline, aniline-NHD and aniline-ND 2, Spectrochimica Acta, 16 (1960) 428-442.

[55] H. Tanak, F. Koçak, E. Ağar, A combined experimental (XRD, FT-IR, and UV–Vis) and DFT computational studies on (E)-N-[4-bromo-2-(trifluromethoxy) phenyl]-1-(5-nitrothiophen-2-yl) methanimine, Molecular Physics, 114 (2016) 197-212.

[56] N.P. Roeges, A guide to the complete interpretation of infrared spectra of organic structures, Wiley, 1994.

[57] S.A. Pourmousavi, A. Kanaani, F. Ghorbani, K.K. Damghani, D. Ajloo, M. Vakili, Synthesis, spectroscopic investigations and computational study of monomeric and dimeric structures of 2-methyl-4-quinolinol, Res Chem Intermed, (2015) 1-38.

[58] B. Kosar, C. Albayrak, Spectroscopic investigations and quantum chemical computational study of (E)-4-methoxy-2-[(p-tolylimino) methyl] phenol, Spectrochimica Acta Part A: Molecular and Biomolecular Spectroscopy, 78 (2011) 160-167.

[59] M. Tezer, S. Kanbul, Opinions of teachers about computer aided mathematics education who work at special education centers, Procedia-Social and Behavioral Sciences, 1 (2009) 390-394.

[60] G.S. Chen, R.S. Talekar, K.T. Wong, L.C. Chi, J.W. Chern, Physical Properties of 8-Substituted 5, 7-Dichloro-2-Styrylquinolines as Potential Light Emitting Materials, Journal of the Chinese Chemical Society, 54 (2007) 1387-1394.

[61] R. Parthasarathi, J. Padmanabhan, V. Subramanian, B. Maiti, P. Chattaraj, Toxicity analysis of 33'44'5-pentachloro biphenyl through chemical reactivity and selectivity profiles, Current Science, 86 (2004) 535.

[62] R. Parthasarathi, J. Padmanabhan, U. Sarkar, B. Maiti, V. Subramanian, P.K. Chattaraj, Toxicity analysis of benzidine through chemical reactivity and selectivity profiles: a DFT approach, Internet Electronic Journal of Molecular Design, 2 (2003) 798-813.

[63] N. Troullier, J.L. Martins, Efficient pseudopotentials for plane-wave calculations, Physical review B, 43 (1991) 1993.

[64] J.P. Perdew, K. Burke, M. Ernzerhof, Generalized gradient approximation made simple, Physical review letters, 77 (1996) 3865.

Table 1: Optimization of reaction conditions[a]

Entry	$SbCl_3$ (gr)	Solvent	Time (min)	Yield (%)
1	0/01	MeOH	80	70
2	0/02	MeOH	40	90
3	0/03	MeOH	3	100
4	0/05	MeOH	3	100
5	0/01	MeOH	3	90
6	---	MeOH	1440	10
7	0/03	---	120	53
8	0/03	DMF	5	92
9	0/03	CH_3CN	50	94
10	0/03	n-Hexane	115	30
11	0/03	DCM	65	60
12	0/03	Ethyl Acetate	90	86
13	0/03	H_2O	50	82
14	0/03	EtOH	5	93

[a] Reaction conditions: 2-aminobezamide (1 mmol), 4-Methyl benzaldehyde (1 mmol), solvent (3 mL), room temperature.

Table 2 Synthesis of 2,3-dihydro-2-arylquinazolin-4(1*H*)-ones promoted by $Sbcl_3$[a]

Entry	Aldehyde or ketone	Product	Time (min)	Yield (%)[b]
1	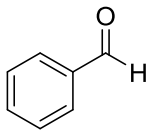 2a	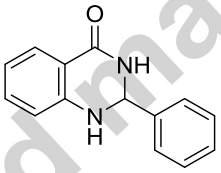 3a	5	95
2	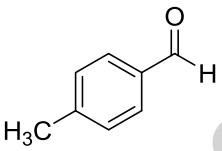 2b	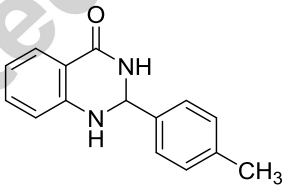 3b	3	97
3	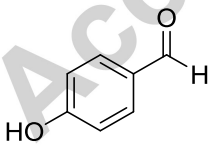 2c	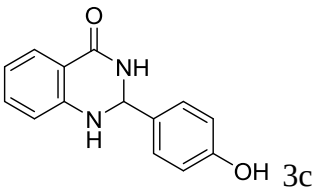 3c	8	92
4	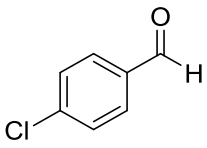 2d	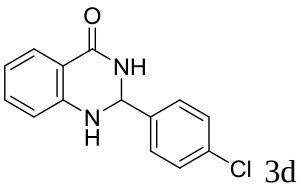 3d	10	96

5	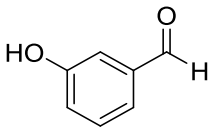 2e	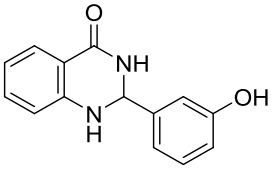 3e	8	92
6	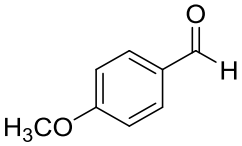 2f	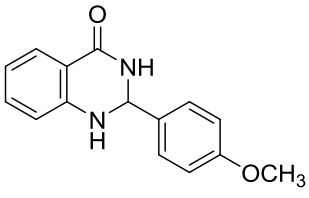 3f	8	98
7	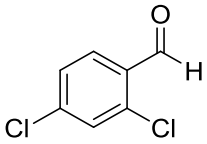 2g	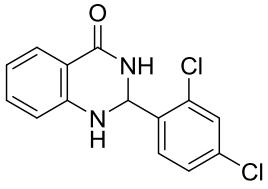 3g	14	94
8	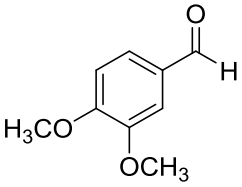 2h	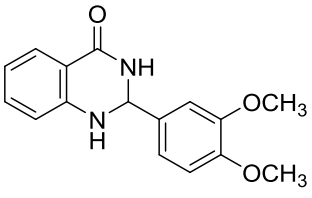 3h	7	96
9	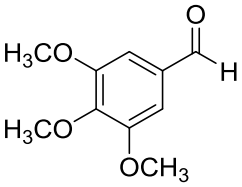 2i	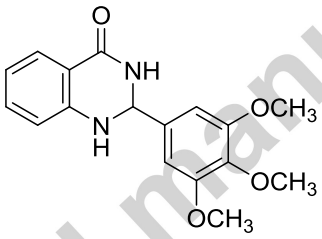 3i	18	97
10	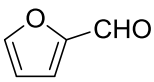 2j	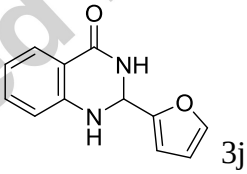 3j	5	90
11	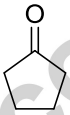 2k	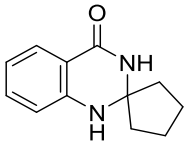 3k	30	88
12	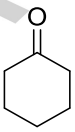 2l	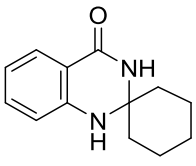 3l	60	93
13	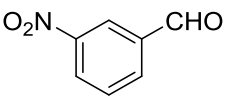 2m	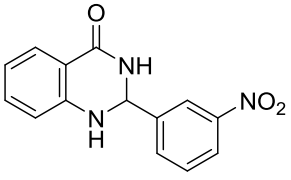 3m	45	98

14	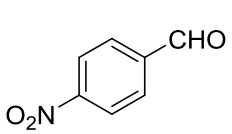 2n	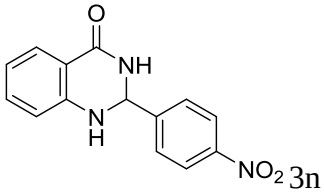 3n	30	98
15	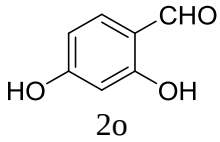 2o	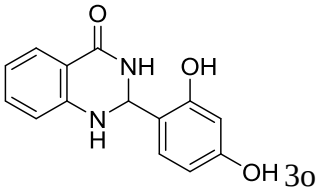 3o	15	94
16	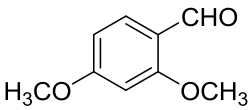 2p	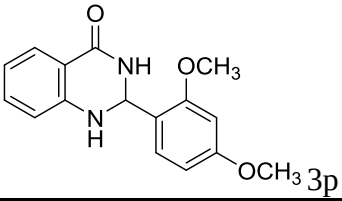 3p	11	97

[a] Reaction conditions: 2-aminobezamide (1 mmol), aldehyde or ketone (1 mmol), solvent (3 mL), room temperature
[b] Isolated yields

Table 3 Comparison results of $SbCl_3$ with recently reported catalyst in the synthesis of 2,3-Dihydroquinazolin-4(1*H*)-ones.

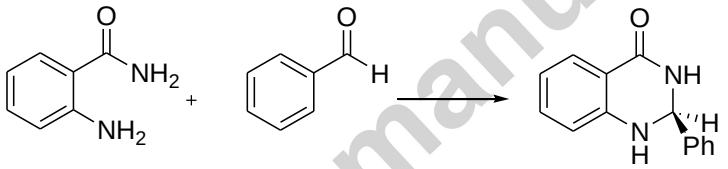

Entry	Catalyst	Conditions[a]	Time	Yield[b] %
1	TBAB	Solvent-free 100 °C	5 min	94
2	$ZrCl_4$	EtOH r.t.	45 min	91
3	$H_3PW_{12}O_{40}$	H2O r.t.	38 min	92
4	Al/Al_2O_3 NPs	Solvent-free 115 °C	15 min	88
9	$SbCl_3$	MeOH r.t.	5 min	90

[a] Reaction conditions: 2-aminobezamide (1 mmol), benzaldehyde (1 mmol) and catalyst under different conditions
[b] Isolated yields

Table 4 Optimized geometrical parameters of PDQ at B3LYP/6-311++G(2d,p) level.

Parameters[a]	Monomer	Dimer	Exp.[b]	Parameters[a]	Monomer	Dimer	Exp.[b]
Bond lengths (Å)							
C_2-C_3	1.400	1.403	1.406	N_{16}-C_{13}	1.460	1.461	1.461
C_3-C_4	1.406	1.409	1.406	C_{13}-H_{29}	1.104	1.105	
C_4-C_5	1.395	1.397	1.397	C_{13}-N_{15}	1.460	1.463	1.458
C_3-N_{15}	1.393	1.389	1.383	C_{13}-C_{18}	1.514	1.461	1.545
N_{15}-H_7	1.011	1.011	0.878	C_{18}-C_{19}	1.393	1.395	1.392
C_4-C_{10}	1.485	1.485	1.478	C_{18}-C_{20}	1.397	1.398	1.400
C_{10}-O_{17}	1.221	1.243	1.247	RN—H	1.011	1.036	0.878
C_{10}-N_{16}	1.379	1.361	1.349	RO…N	---	2.871	2.846
				RH…O	---	1.770	1.970
Bond angles (°)							
A(2,3,4)	119.2	119.2	122.4	A(14,16,13)	117.1	118.0	115.1
A(2,3,15)	121.6	122.1	122.4	A(10,16,14)	114.6	116.4	119.9
A(3,4,5)	119.9	120.0	120.1	A(10,16,13)	121.7	122.0	121.9
A(3,4,10)	119.9	119.4	119.1	A(15,13,16)	106.9	107.6	106.8
A(3,15,13)	116.4	116.9	117.5	A(15,13,18)	111.2	110.6	111.4
A(3,15,7)	114.7	115.5	118.4	A(15,13,29)	110.0	109.8	
A(4,10,17)	123.9	122.1	122.4	A(16,13,18)	111.2	111.6	110.9
A(16,10,17)	121.7	122.3	121.9	A(13,18,19)	120.1	120.1	119.0
A(4,10,16)	114.3	115.6	115.7	A(N–H…O)	---	175.2	174.4
Dihedral angles (°)							
D(2,3,15,13)	153.1	153.2	155.4	D(17,10,16,13)	-161.1	-165.7	−165.49
D(2,3,4,10)	176.4	175.6	171.9	D(10,16,13,15)	-48.8	-44.5	−45.85
D(3,4,10,17)	-171.8	-169.1	−166.39	D(3,15,13,18)	172.8	172.2	167.0
D(3,4,10,16)	5.4	8.5	11.1	D(10,16,13,18)	-170.4	-166.1	−163.94
D(4,3,15,13)	-29.6	-29.7	−26.98	D(13,18,20,23)	-179.8	179.5	-179.9
D(4,10,16,13)	21.6	16.7	17.0	D(16,13,15,3)	51.3	50.1	50.0
D(5,4,10,16)	-177.8	-175.5	-174.3	D(16,13,18,19)	-117.8	-120.1	127.9
				D(15,13,18,20)	-56.9	-59.4	−53.28

[a] For atom numbering from Fig. 2.

[b] Ref.[51]

Table 5 Experimental (FT-IR wavenumbers (in cm^{-1})) and theoretical (scaled wavenumbers (in cm^{-1})) of PDQ at B3LYP/6-311++G(d,p) and B3LYP/6-311++G(2d,p) level of theory.

B3LYP/6-311++G(d,p			B3LYP/6-311++G(2d,p)				
Freq	I.IR	A_R	Freq	I.IR	A_R	IR (Neat)	Vibrational assignments (PED)
3601	37	96	3438	37	94	3301(31)	$\upsilon N_{16}H_{14}$(100)
3590	16	95	3423	15	93	3178(20)	$\upsilon N_{15}H_{7}$(100)
3199	10	210	3056	10	204	3131(17)	$\upsilon_s CH_I$(96)
3193	7	286	3051	7	294	3057(16)	$\upsilon_s CH_{II}$(96)
3187	18	99	3045	17	89	3035(13)	$\upsilon_a CH_{II}$(99)
3177	15	102	3035	14	101	2936(10)	$\upsilon_a CH_{II}$(100)
3173	12	114	3032	11	115	2902(9,sh)	$\upsilon_a CH_I$(95)
3156	7	57	3016	7	56	2850(7)	$\upsilon_a CH_I$(93)
2904	78	105	2774	76	103	2804(7)	$\upsilon C_{13}H_{29}$(100)
						1813(2)	Overtone/combination
						1884(3)	Overtone/combination
						1910(4)	Overtone/combination
						1950(4)	Overtone/combination
1741	536	55	1726	510	55	1671(57)	$\upsilon C{=}O$(77)
1650	168	47	1642	155	46	1660(40)	υCC_I(38), δCH_I(15), $\upsilon_a C_4$-$C_{10}{=}O_{17}$(11)
1644	0	45	1638	0	45	1649(63)	υCC_{II}(48), δCH_I(21)
1628	0	11	1621	0	11	1613(64)	υCC_{II}(40)
1620	4	12	1612	4	12	1587(12,sh)	$\upsilon_a CC_I$(34), $\delta N_{15}H_7$(12)
1523	153	6	1520	61	5	1510(45)	δCH_I(24), $\upsilon_a CC_I$(14), δNH(14)
1514	197	2	1509	254	2	1484(37)	δCH_I(22), νC_3-N_{15}(12), $\upsilon_a CC_I$(11)
1491	23	3	1490	23	2	1454(18)	δCH_I(42), $\delta C_{13}H_{29}$(15)
1469	46	18	1466	61	19	1439(25)	δNH(28), δCH_I(18), υ_sNCN(10)
1436	71	10	1430	67	9	1424(9,sh)	δNH(28), $\delta C_{13}H_{29}$(25), $\upsilon_a C_4C_{10}N_{16}$(10)
1393	11	5	1390	13	4	1384(22)	δCH_{II}(43), $\delta C_{13}H_{29}$(21)
1373	167	10	1369	170	9	1362(16)	δNH(19), δCH_I(14), $\delta C_{13}H_{29}$(14)
1349	10	8	1342	27	19	1327(14)	$\upsilon_a CC_I$(36)
1316	25	1	1310	23	1	1301(29)	$\upsilon_a CC_{II}$(21), $\delta C_{13}H_{29}$(13)
1306	62	15	1299	62	15	1284(8)	$\delta C_{13}H_{29}$(19), $\upsilon_a C_4C_{10}N_{16}$(15), δNH(14)
1279	4	25	1275	5	20	1257(7)	δCH_I(22), υC_3N_{15}(16), $\delta C_{13}H_{29}$(10)
1248	2	33	1242	2	35	1239(6)	υCN(34), $\delta C_{13}H_{29}$(14)
1198	5	5	1196	5	5	1206(3)	δCH_{II}(95)
1183	0	3	1180	0	3	1169(15)	δCH_{II}(68), $\upsilon_a CC_{II}$(19)
1181	14	8	1178	13	8	1158(6)	δCH_I(64)
1167	27	2	1161	30	2	1149(16)	$\nu_a C_{10}$-N_{16}-C_{13}(31), δCH_I(26)
1149	34	7	1143	31	8	1134(9)	ν_aN-C-N(50), δCH_I(11)
1114	1	6	1112	1	6	1119(3)	δCCC_I(35), δCH_I(13)

1105	3	0	1101	3	0	1095(2)	$\nu_a CCC_I(38)$, $\delta CH_I(38)$
1055	7	39	1051	6	40	1075(3)	Ring breathing $_I(64)$
1048	13	10	1045	12	8	1035(5)	Ring breathing $_{II}(82)$
1018	1	40	1018	0	46	1027(8)	Trigonal bending $_{II}(85)$
1012	9	16	1006	8	14	1003(4)	$\nu_s NCN(57)$
996	0	0	987	0	0	985(3)	$\gamma CH_I(79)$
991	0	0	981	0	0	969(2)	$\gamma CH_{II}(89)$
975	1	0	966	1	0	950(3)	$\gamma CH_I(80)$
942	5	0	938	5	0	940(3)	$\gamma CH_I(78)$
913	6	6	913	5	6	922(6)	$\delta CCC_I(24)$, $\delta CCC_{II}(14)$, $\delta NCN(11)$
870	4	0	866	5	1	911(7)	$\gamma CH_I(70)$
853	2	3	851	2	3	852(4,sh)	$\delta CCC_I(19)$, $\delta CCC_{II}(15)$, νC_{13}-$C_{18}(10)$
803	2	0	798	2	0	811(28)	$\gamma C_4C_{10}O_{17}(45)$, $\gamma CH_I(13)$
790	53	14	790	58	11	793(3)	$\delta NCN(35)$
782	32	1	780	27	2	772(4,sh)	$\gamma CH_{II}(44)$, $\gamma CCC_{II}(12)$
767	54	2	762	50	2	747(57,sh)	$\gamma CH_I(73)$, $\gamma CCC_{II}(11)$
744	3	9	743	3	9	727(57)	$\delta CCC_I(25)$, $\delta C3C_4C_{10}(11)$, $\delta NCN(10)$
714	45	0	712	45	0	699(37)	$\gamma CH_{II}(59)$
707	29	1	705	30	1	685(18)	$\gamma C_4C_{10}N_{16}(34)$, $\gamma CCC_{II}(28)$
660	2	5	660	2	5	664(34)	$\delta CCC_{II}(18)$, $\delta CCC_I(13)$
618	31	3	621	39	5	641(25)	$\gamma NH(20)$, δO=C-N(16)
598	2	7	599	3	7	621(3,sh)	δO=C-N(16), $\gamma NH(12)$, $\delta C_{10}N_{16}C_{13}(10)$
571	47	2	571	45	2	600(10)	$\gamma NH(50)$
551	124	1	556	132	1	565(7)	$\gamma NH(53)$
540	24	1	539	11	1	529(16)	$\gamma CCC_3N_{15}(10)$
498	19	2	497	16	2	508(10)	$\delta NCN(15)$, $\gamma CCC_{II}(10)$
481	2	2	479	3	2	490(19)	$\gamma NH(30)$, $\gamma CCC_{II}(11)$
449	5	6	449	3	6	461(3)	$\delta CN_{15}C(25)$, $\gamma NH(13)$

Freq, vibrational wavenumber; I.IR, IR intensities in kM/mol; AR., Raman scattering activities in A**4/AM; experimental relative intensities are given in parenthesis; sh, sholder; s, symmetric; a, asymmetric υ, stretching; δ, in-plane bending; γ, out-of-plane bending.

Table 6 Comparing several properties related to the hydrogen bond strength (O…H–N) for PDQ and 2MQ (All calculated at the B3LYP/6-311++G(2d,p) level).

	PDQ	2MQ [d]
Geometrical results[a]		
RO…N	2.871	2.887
RN–H	1.036	1.027
O…H	1.770	1.864
θ N–H…O	175.2	174.1
AIM results[b]		
ρ_{BCP}	0.0484	0.0309
$\nabla^2\rho_{BCP}$	0.0279	0.0228
H_{BCP}	-0.0076	-0.0001
H-bond energy	13.5384	7.0837
Spectroscopic results[c]		
νNH	3438 (3301)	3610 (3426)
γNH	571 (600)	437 (435)

[a] R is the intramolecular O…N, N–H, O…H distances in Å, θ: the hydrogen bond angle N-H…O in degree.

[b] The units of AIM results are: ρ_{BCP} (e au^{-3}), $\nabla^2\rho_{BCP}$ (e au^{-5}), H_{BCP} (hartree au^{-3}) and H-bond energy (kcal/mol).

[c] ν and γ are stretching and out-of-plane bending modes frequencies, respectively, in cm^{-1}. (Experimental values are given in parenthesis).

[d] Data source: Ref.[57]

Table 7 For keto and enol1 forms wavelength, oscillator strength, major contributions of calculated transitions in gas phase and various solvents.

	Exp.	Calculated (keto-amine)			Calculated (enol-imine)		
	λ (nm)	λ (nm)	*f*	Major contribution	λ (nm)	*f*	Major contribution
THF	**368**				**340**	0.049	H→ L+1(98%)
	321	322	0.055	H→ L(97%)			
	273	271	0.025	H→ L+1(95%)	274	0.031	H→ L(93%)
	237	240	0.032	H→ L+4(75%), H→ L+5(0.09%)	250	0.063	H→ L+4(55%), H-1→ L(28%)
CH_3CN					340	0.047	H→ L(98%)
	330	324	0.055	H→ L(97%)			
	261	270	0.024	H→ L+1(96%)	274	0.029	H→ L+1(93%)
	219	239	0.061	H→ L+4(46%), H-2→ L(20%), H-1→ L(12%)	249	0.059	H→ L+4(49%), H→ L+1(27%), H→ L+3(11%)

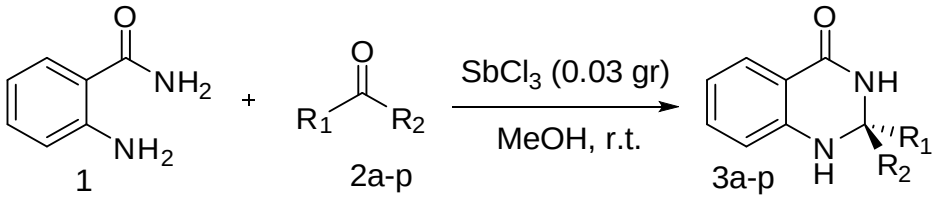

Scheme. Synthesis of 2,3-Dihydroquinazolin-4(1*H*)-ones catalyst by $SbCl_3$

Fig. 1. Tautomeric forms for (PDQ); I: keto-amine, II: enol-imine, and III: enol-amine.

Fig. 2. The theoretical optimized geometric structure with atoms numbering of PDQ.

Fig. 3. Comparison of observed and calculated IR spectra of PDQ (a) observed; (b) calculated with B3LYP/6-31++G(2d,p).

Fig. 4. Molecular electrostatic potential map (MEP) of PDQ.

Fig. 5. The atomic orbital compositions of the frontier molecular orbital for PDQ.

Fig. 6. UV-Vis absorption spectra of PDQ in different solvents.

Fig. 7. TG and DTG curves of PDQ.

Fig. 8. Calculated current–voltage (*I*–*V*) characteristics for OFF and ON state structures of PDQ.

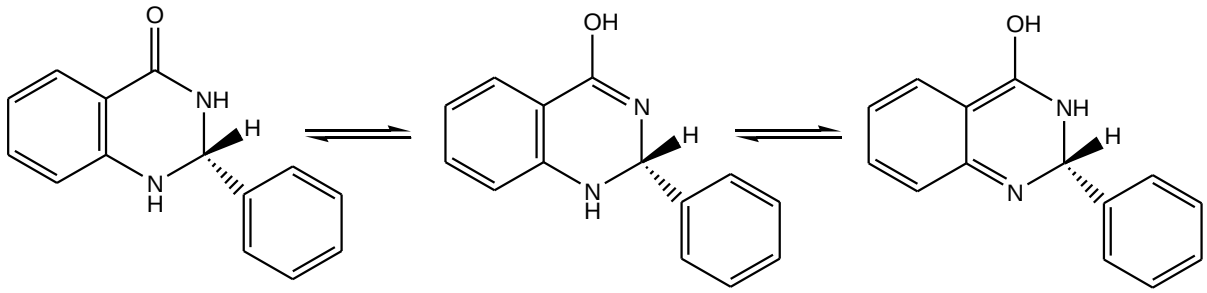

Fig. 1

2

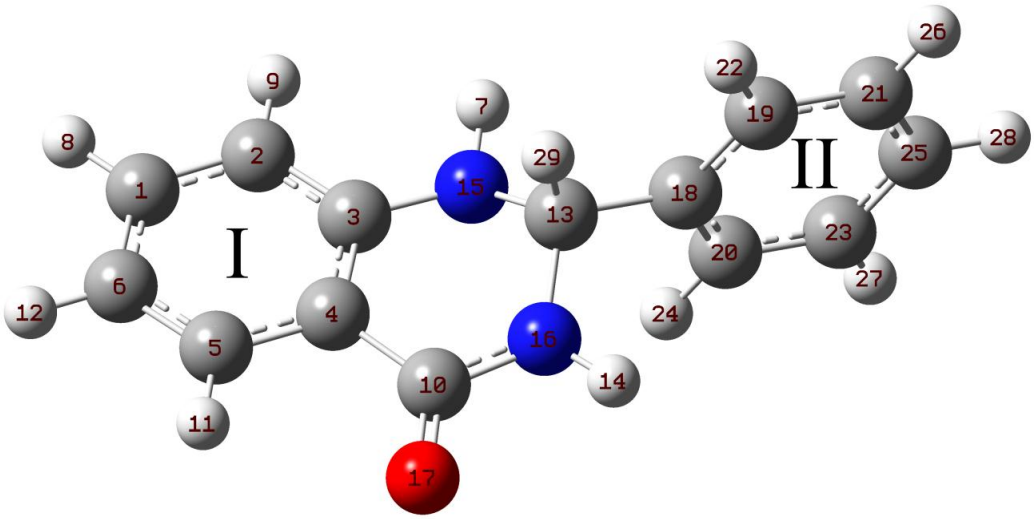

Fig. 2

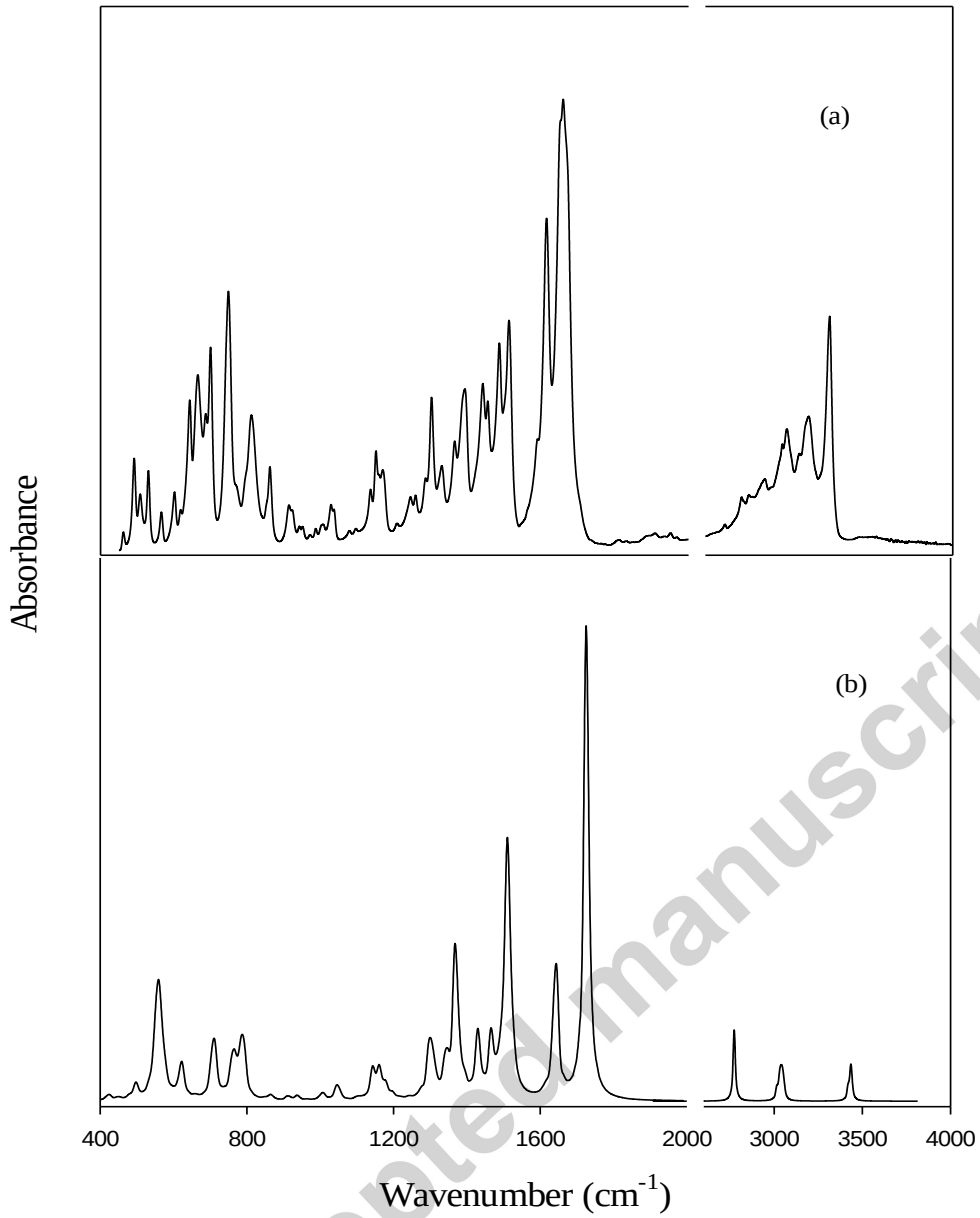

Fig. 3

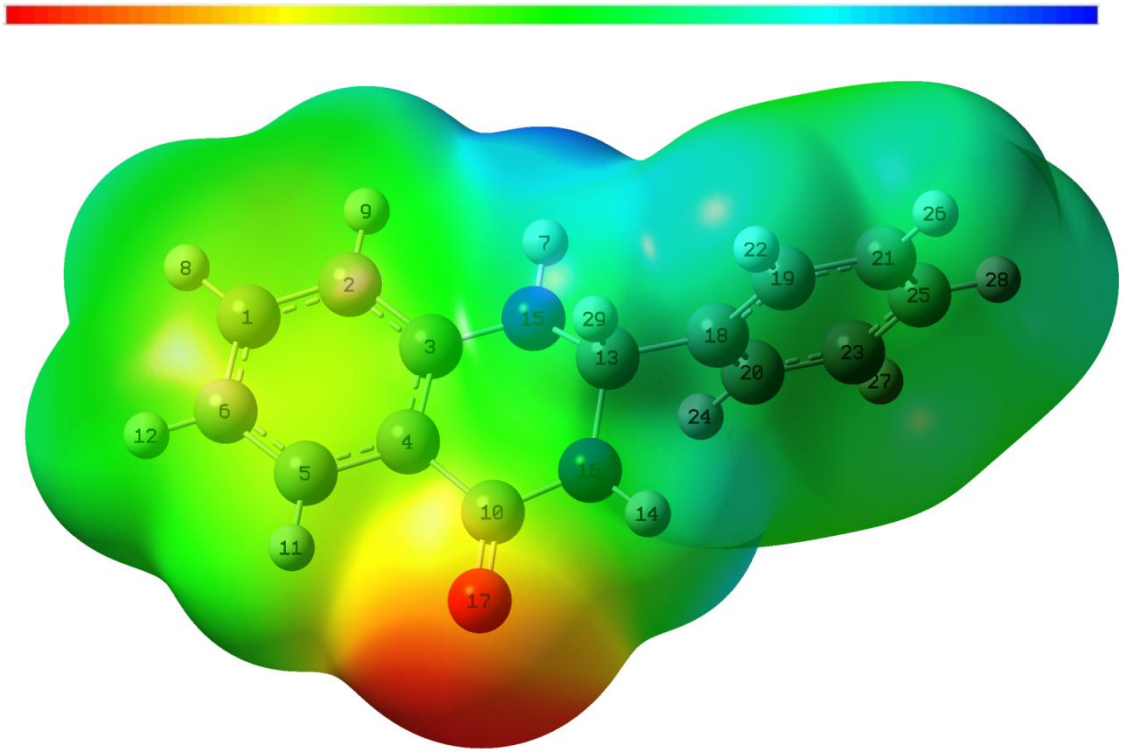

Fig. 4

Atom	Charges (e)	Electric Potential (a.u)
C_1	-0.164	-14.763
C_2	-0.251	-14.767
C_3	0.206	-14.718
C_4	-0.193	-14.765
C_5	-0.134	-14.769
C_6	-0.240	-14.776
H_7	0.381	-1.017
C_{10}	0.677	-14.673
C_{13}	0.177	-14.673
H_{14}	0.400	-1.018
N_{15}	-0.623	-18.366
N_{16}	-0.649	-18.370
O_{17}	-0.618	-22.410
C_{18}	-0.072	-14.748
C_{19}	-0.191	-14.755
C_{20}	-0.181	-14.759
C_{21}	-0.199	-14.757
C_{23}	-0.195	-14.758
C_{25}	-0.193	-14.758
H_{29}	0.160	-1.104

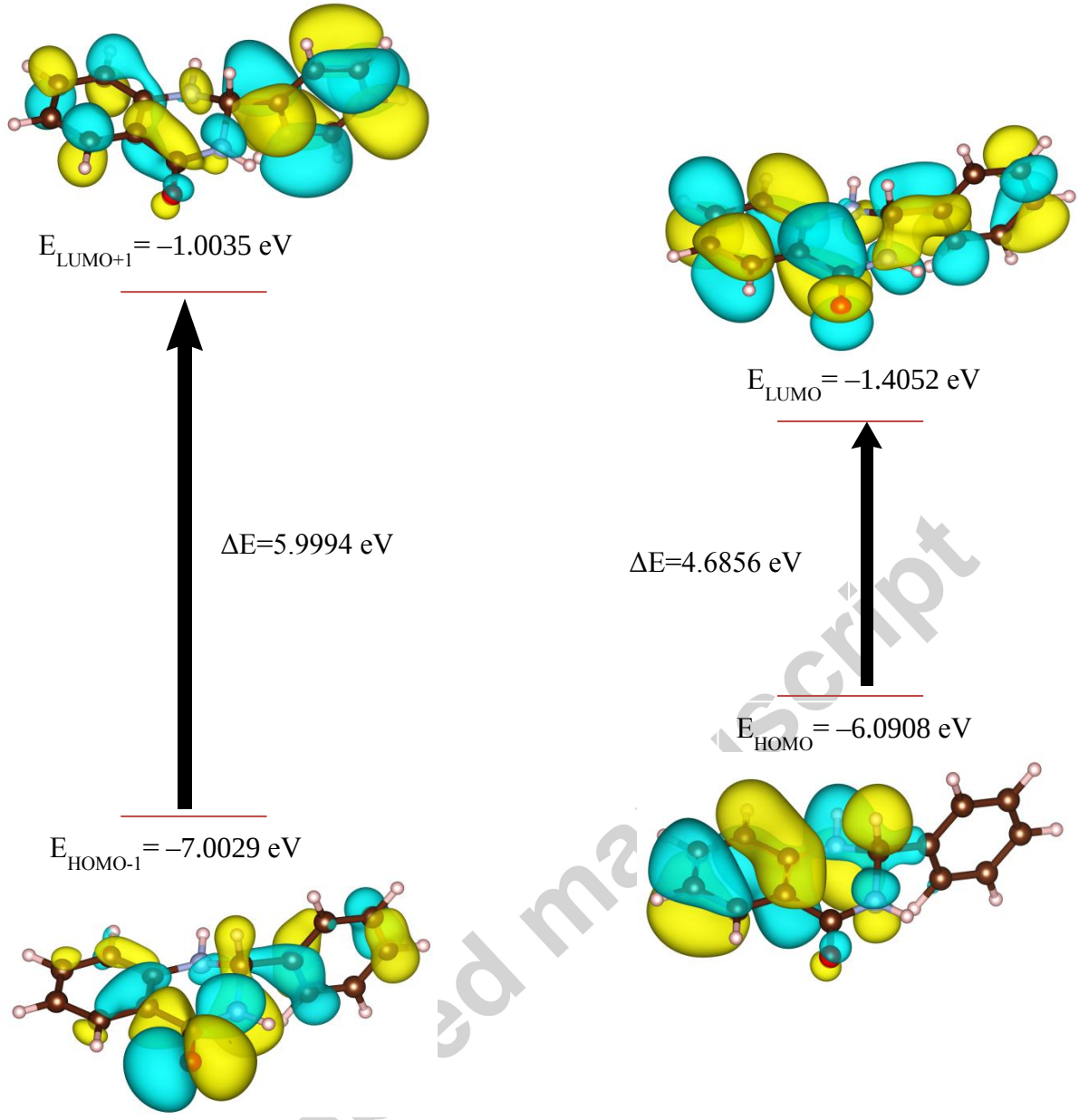

Fig. 5

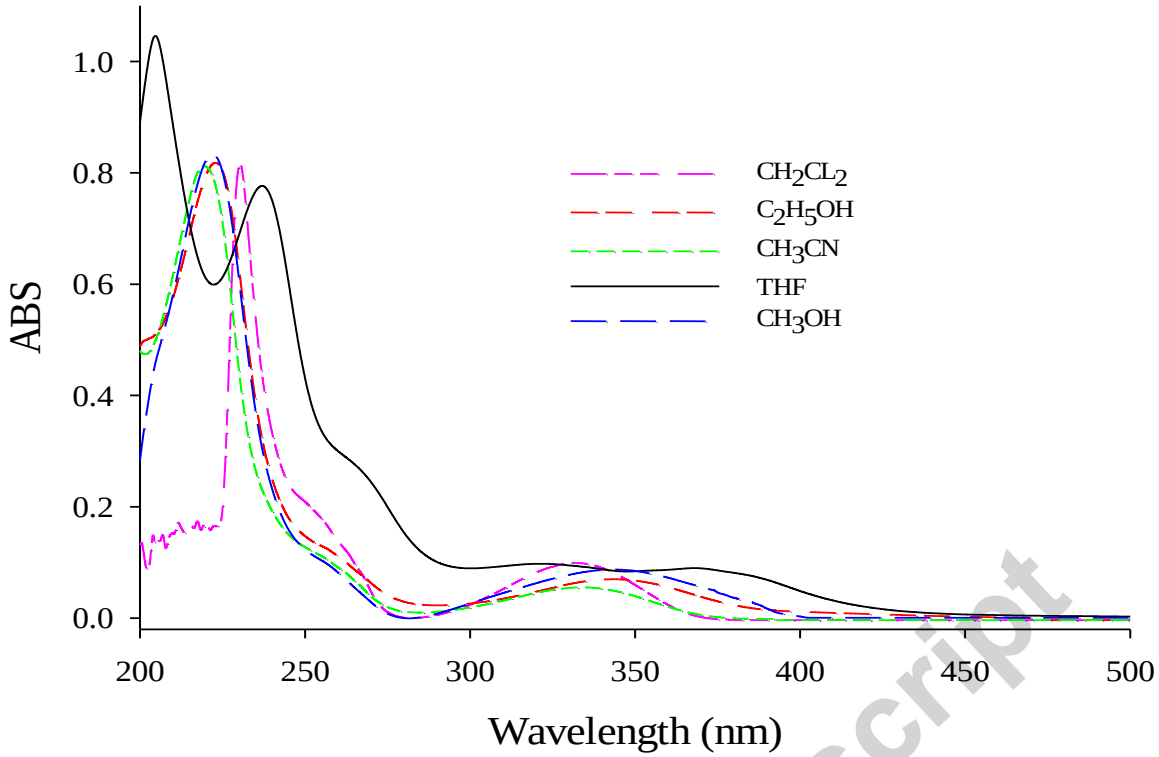

Fig. 6

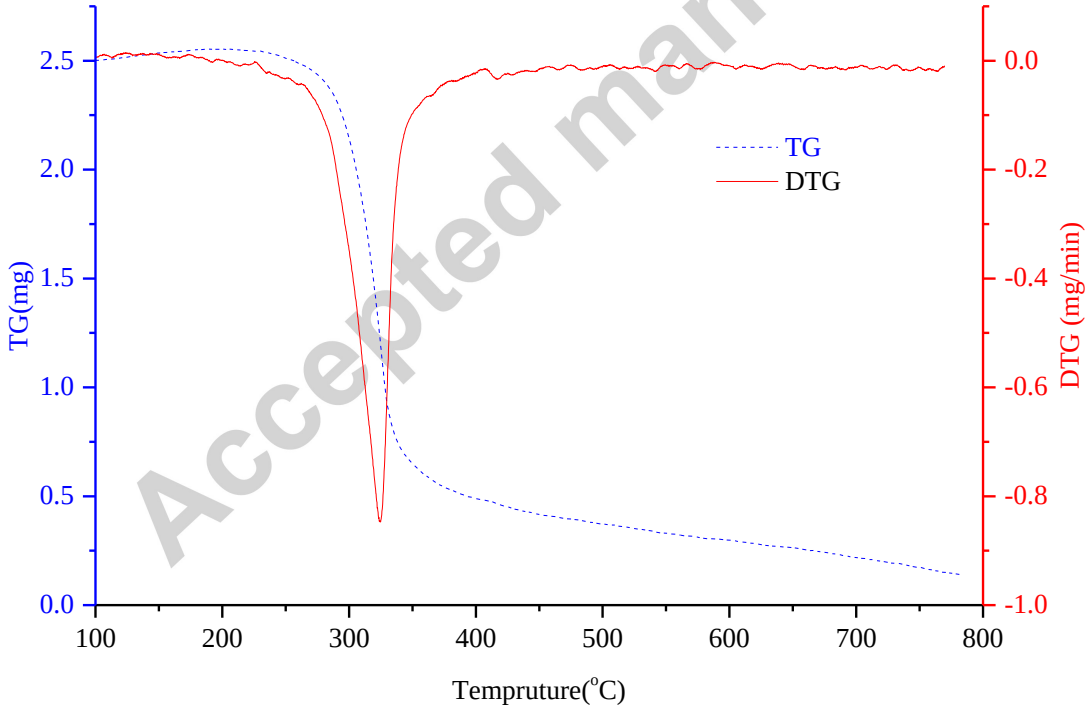

Fig. 7

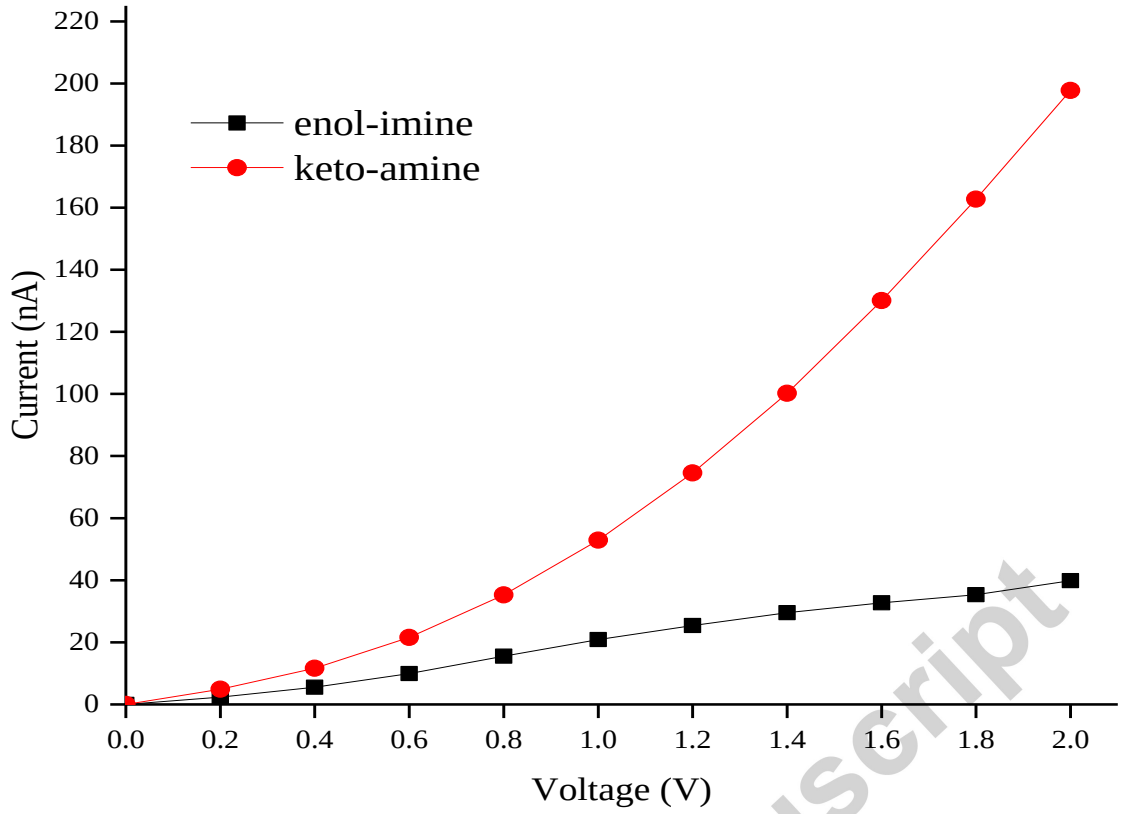

Fig. 8

Highlights

- The synthesis of quinazolines was carried out by $SbCl_3$ as efficient and green catalyst.
- Proton tautomerism is experimentally and theoretically investigated.
- The hydrogen bond in PDQ is stronger than that in 2MQ.
- Transition structures were calculated by QST3 approach and IRC calculation yielded.
- Title compound has been proposed as a potential molecular electronic device.